EIFEL: An Experiment on Tube Array Instability at High Reynolds Number

P. Caumette, J. L. Garcia, F. Lambert
CEA-CEN, St. Paul-lez-Durance, France
G. Chevereau
FRAMATOME, Paris la Defense, France

ABSTRACT

The EIFEL experiment was designed to investigate the stability of a dense array of tubes in crossflow, at a high, supercritical Reynolds number.

The phenomenon proved not to be of pure fluidelastic type. The effect of high Reynolds (in fact of a lower viscosity), if any, is small.

INTRODUCTION

Among PWR structural components, the control rod guiding tubes form, in the upper plenum of the core, a very dense array with a reduced pitch-to-diameter ratio. The crossflow velocity is at places very high, close to the critical velocity one can deduce from a Connors fluidelastic instability model (Blevins, 1977). It was therefore necessary to insure that no instability of the tube bundle had to be feared, particularly in an unexplored domain (around 2.10^7) of the Reynolds number.

To assess the safety margin, FRAMATOME and the Commissariat à l'Energie Atomique jointly undertook an experimental program, the main part of which is the EIFEL experiment.

THE EIFEL EXPERIMENT

The rod array is represented by a 14 tube bundle, with a pitch of 75.3 mm, 63.3 mm in diameter. To obtain the large velocities required without recurring to large pumps, our idea was to use the discharge of a large pressurized vessel (10 m^3) through the mock-up. We used the SUPER CLAUDIA facility (fig. 1 and 2), which has been designed to test different sorts of valves in reactor conditions (365°C, 220 bar). It allows to maintain a high velocity flow (> 40 m/s) through the mock-up during an effective time of about 2.5 s. This is large enough, compared to the vibration period (around 5 ms) of the rods.

The complete assembly is presented on fig. 3. The flow is guided through an 8° diverging nozzle and ten dummy rigid rods before entering the active chamber. The 14 rods plunging in the latter are built in a support plate at the upper end and free at the lower one (fig. 4). The triangular array is completed by dummy rod parts on the walls (fig. 5).

The rod rows are oriented parallel to the flow, as they would be in actual configuration. The discharge is initiated by activating a fast opening valve, downstream of the mock-up. A profiled nozzle has been placed in front of the valve, to report at that point an eventual flashing of the water.

The rods are equipped with a total of 20 strain gauges and accelerometers in both x and y directions. The sampling frequency is about 1 kHz for each transducer.

Prior to the experiment, the rods are set in tune by adjusting a moveable masslet at their free end. In order to characterize each tube separately, the following procedure was used : the tubes were adjusted one at a time, the rest of the bundle being rigidified by inserted wedges.

THE PROGRAM

Two sets of tubes were tested, differing by their lengths (300 and 450 mm). Instability could only be reached with the longer ones.

VIBRATION OF THE SHORT TUBES

Tube frequencies were adjusted between 410 and 420 Hz in air. Rod characteristics, frequency f and relative damping ε, as measured in air and in still water, are given in table 1.

TABLE 1 - Short tube characteristics

	Air	Water
f(Hz)	415±5	355
ε (%)	0.15	0.6

Fig. 6 shows a typical velocity variation during an experiment. The signal delivered by the transducers was analysed during a time interval of 1 s, near the maximum, where the velocity can be considered as constant. The amplitude spectra for accelerometer A1 (tube n°5, x direction) presented, after convenient smoothing, on fig. 7, show that they are quite insensitive to the velocity level. Two large peaks are observed, one of which, around 360 Hz, corresponds to the individual rod frequency.

The power of the signal, when plotted versus the velocity in a log-log representation (fig. 8), shows a linear variation, with slope 4.9. This is in agreement with tube vibration under a turbulent excitation source of the Dryden type, with an exponent of 2. There is no indication that any instability was approached, even at the largest (52 m/s) intertube velocity attained.

As a side result, the stationary component of the strain gauge signal provides an estimation of rod drag coefficient : variable from one tube to another, its maximum value is obtained on the row before last (rod n°7) : $C_X = 0.31 \pm 0.03$.

VIBRATION AND INSTABILITY OF THE LONG TUBES

The tests were repeated in the same configuration but with longer (450 mm) tubes. The rod length affected by the flow is still 300 mm. Measured characteristics are given in table 2.

TABLE 2 - Long tube characteristics

	Air	Water
f(Hz)	208±2	180
ε (%)	0.15	0.4

With such lowered frequency, the instability could be attained : this is evidenced by fig. 9, which represents the signal delivered by a strain gauge during a test at room temperature (20°C). Successive time intervals of 0.1 s were analysed for three strain gauges and the average signal power plotted against velocity (fig. 10). Also plotted on the figure are similar results obtained during a stable test (maximum velocity : 40 m/s). Successive 0.5 s time intervals were analysed on the pseudo-plateau following the

maximum. A sharp transition is visible between the vibrational regime (slope 4.6) and the instability. This means that instability appears with a very short time constant and confirms the validity of such pseudo-static experiments to determined the critical velocity. The critical intertube velocity thus measured is 45 $\pm$ 1 m/s.

INFLUENCE OF TEMPERATURE

Complementary tests were made at higher temperatures to check the influence of Reynolds number. Unfortunately, due to difficulties with the ultrasound flowmeter, velocity measurement at 200°C were only approximate. The results are reported on table 3.

TABLE 3 - Critical velocity variation with temperature

T	20°C (Re=2.8x10^6)	100°C (Re=10^7)	200°C (Re=1.4x10^7)
V m/s	45 $\pm$ 1	43.5 $\pm$ 1	38.5 $\pm$ 2.5

Critical velocity is not significantly reduced at 100°C, but is about 15 % lower at 200°C.

COMPLEMENTARY RESULTS

Tube behaviour during instability

In most cases, due to the strong agitation of the tubes, these were rapidly loosened from their attach on the upper plate, so that only their entry into instability could be observed.

In the few tests we shall now describe, the tubes, more solidly fixed to the support plate, sustained the whole instability period.

For a test performed at 100°C (test n°19), whose flow history is given on fig. 11, instability appeared at the maximum flow velocity (42.8 m/s) and lasted until the velocity was 32.5, well below the critical value.

Moreover, during the instability period, all the tubes vibrate at the same frequency, but this frequency varies with time. This can be seen on the time-spectrum analysis of one of the gauge signals given on fig. 12. Each individual spectrum is obtained on a .23 s time interval. The rod frequency clearly has the same linear variation as the velocity, with the relationship :

$$\frac{fD}{U} = 0.23 .$$

This double phenomenon, outlet velocity much lower than inlet one, correlation between flow velocity and rod vibration, is the sign of a strong coupling between flow and the rod bundle.

Vibration of one isolated tube

When one tube only is allowed to vibrate (tube n°9), the other ones being simply supported at their lower end, the instability of this unique tube is reached at the velocity of 46.5 m/s. Even a single rod is thus subject to instability. The same frequency shift phenomenon can be observed on fig. 13.

Vibration of the bundle, with the tubes out of tune

When tube frequencies are dispersed over a 48 Hz interval (f = 204 $\pm$ 24 Hz in air) the instability is reached at 42 m/s. There is thus no significant effect of detuning on the critical velocity.

The spectral analysis shown fig. 14 indicates that the shift was indeed the rule in all our tests.

Comparison with literature

How do our results compare with published experimental data ? Chen (1982) gives an empirical correlation for "rotated triangular arrays", between reduced critical velocity $U_r = U/fD$ and mass damping parameter $\delta_m = 2\pi\varepsilon m/\rho D^2$.

m, effective mass per rod unit length, was obtained by :

$$m = \frac{\int_o^L m(z)\,\varphi^2(z)\,dz}{\int_o^L \varphi^2(z)\,dz},$$

where $\varphi(z)$ is the tube vibration mode,
m(z) is the rod mass per unit length, taking into account the mass of water inside the tube and an added mass m_a due to surrounding water, which, according to Blevins (1977), is twice the displaced water for such a close array :

$$m_a = 2\,\frac{\pi D^2}{4}\,\rho.$$

U, standard intertube flow velocity, has to be calculated by :

$$U = \frac{P}{P - D}\,U_a \quad (U_a \text{ approach velocity}).$$

This means a 25 % increase on all velocity figures given in this paper.

For the two phases of the experiment,
the tube bundle was not unstable with :

$$\delta_m = 0.21 \qquad U_r = 2.9,$$

and was unstable with :

$$\delta_m = 0.15 \qquad U_r = 4.9.$$

The corresponding points are placed on the diagram, fig. 15.

One sees that our results compare well with available experimental data.

CONCLUSION

. By its characters :

- no significant effect of detuning,
- possibility for one tube to be instable by itself,

the instability evidenced on EIFEL confirms to be more of the "fluid damping controlled" type, as had to be expected with a mass damping parameter lower than one ; it is in good agreement with other experimental data.

. There is but limited influence (some 15 % at 200 °C) of temperature on critical velocity.

. At instability, a particular flow-structure coupling effect has been observed, where the rods have their frequency imposed by the flow.

REFERENCES

Blevins, R.D. (1977). Flow induced vibration. Van Nostrand Reinhold, New York.

Chen, S.S. (1982). The instability flow velocity of tube arrays in crossflow. Int. conf. on flow induced vibration in fluid engineering, Reading, England.

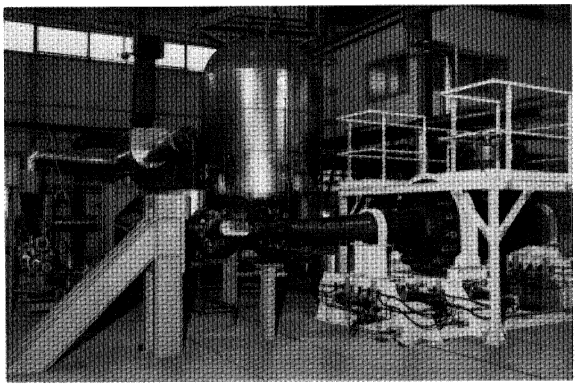

Fig. 1 - A view of SUPERCLAUDIA and the mock-up

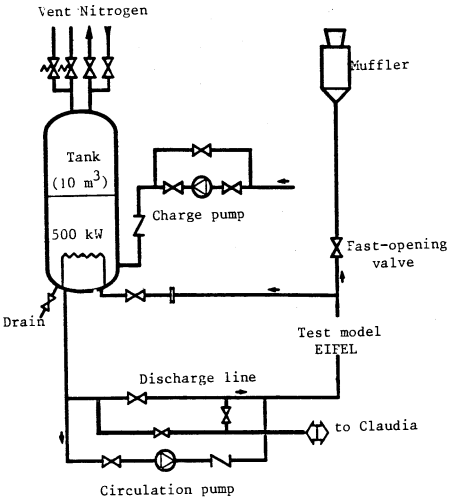

Fig. 2 - SUPERCLAUDIA set-up

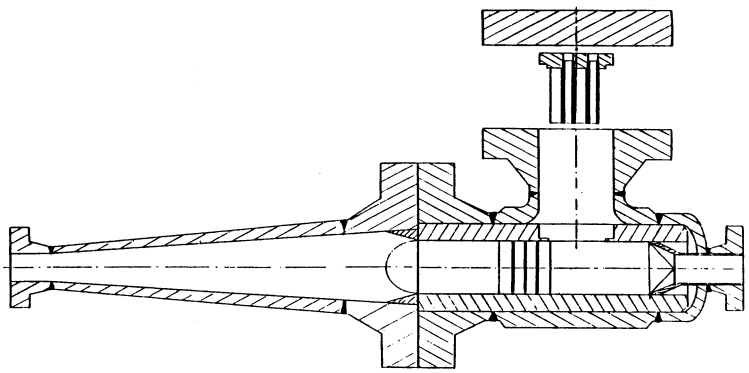

Fig. 3 - Mock-up assembly

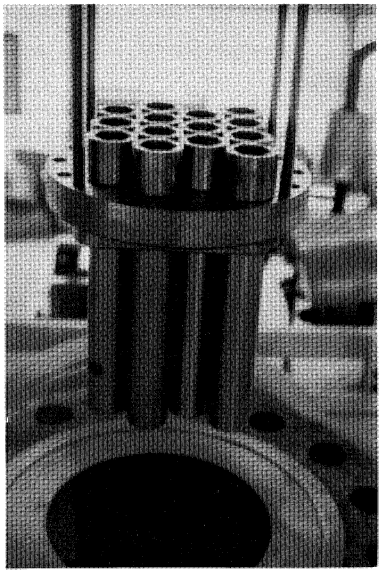

Fig. 4 - A view of the 14-rod bundle

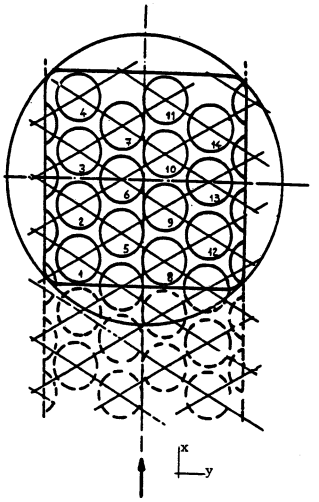

Fig. 5 - Configuration of tube array

Fig. 6 - Flowrate variation vs time

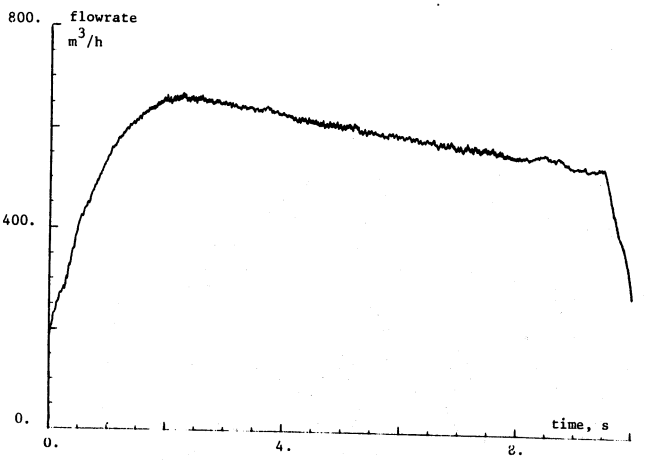

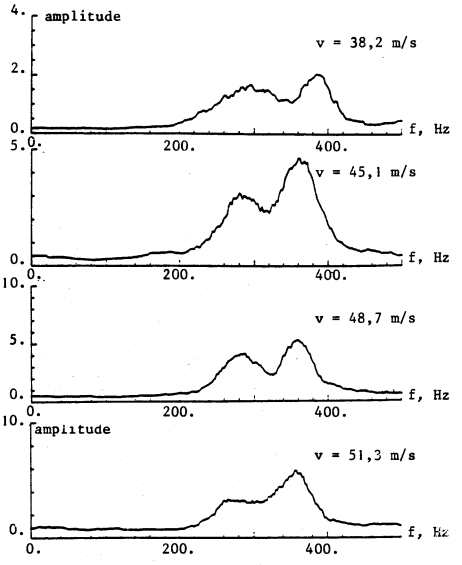

Fig. 7 - Amplitude spectra of accelerometer for different flow velocities

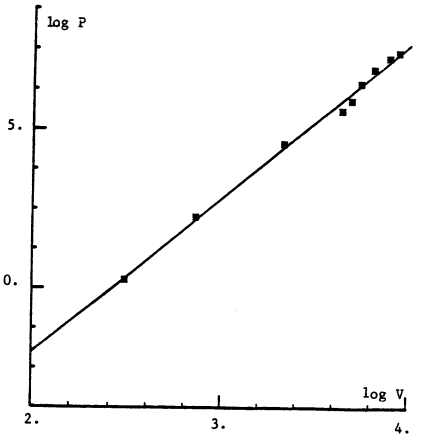

Fig. 8 - Evolution of accelerometer signal power with flow velocity (1st phase)

Fig. 9 - Strain gauge signal showing instability

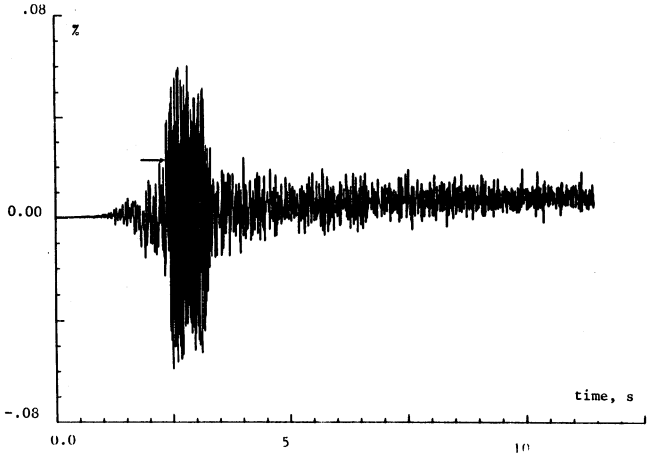

Fig. 10 - Variation of strain-gauge signal power vs velocity (2^d phase)

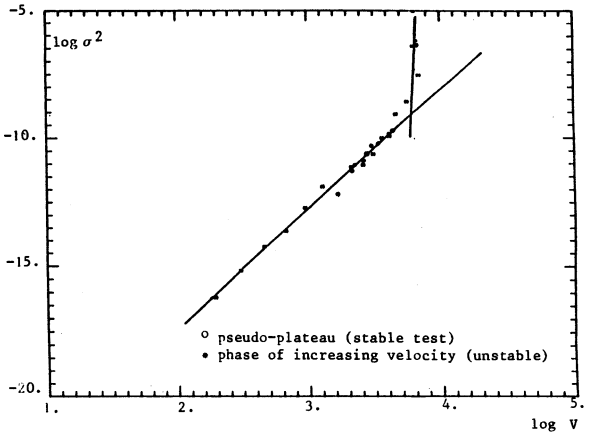

Fig. 11 - Flow history for test # 19

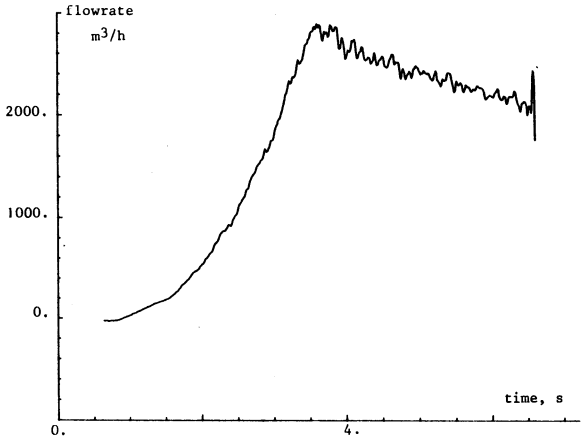

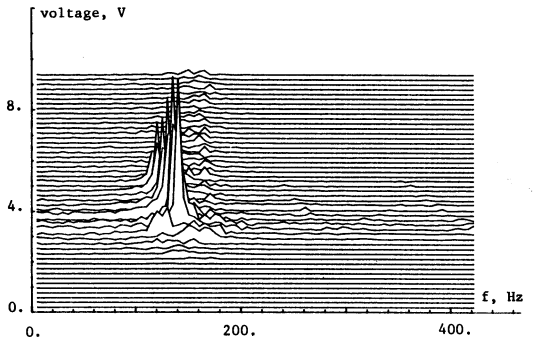

Fig. 12 - Time spectrum analysis for test ≠ 19

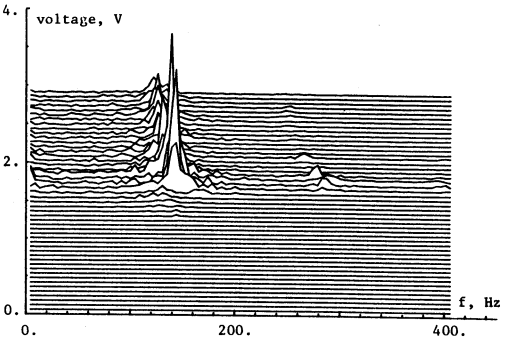

Fig. 13 - Time spectrum analysis : one free rod

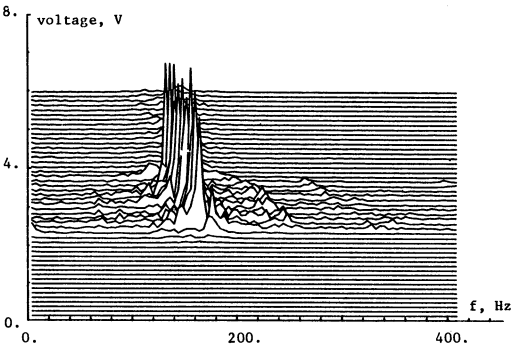

Fig. 14 - Time spectrum analysis : rods out of tune

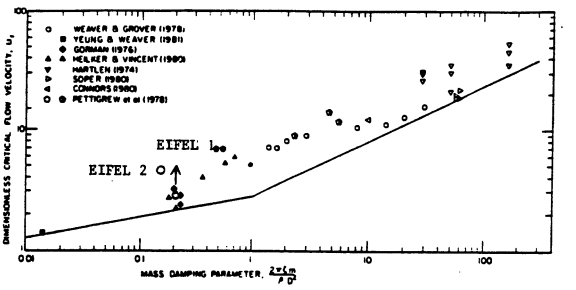

Fig. 15 - Chen's empirical correlation